Journal of Sound and Vibration (2000) **231**(3), 537–548
doi:10.1006/jsvi.1999.2543, available online at http://www.idealibrary.com on IDEAL®

THE EFFECTS OF TRANSVERSE PROFILE ON THE EXCITATION OF WHEEL/RAIL NOISE

D. J. THOMPSON

Institute of Sound and Vibration Research, University of Southampton, Highfield, Southampton SO17 1BJ, England

AND

P. J. REMINGTON

BBN Technologies, 10 Moulton St., Cambridge, MA 02138, U.S.A.

(*Received in final form 23 September* 1999)

At the Fifth International Workshop on Railway Noise in 1995, two papers reported apparently conflicting results relating to the effects of transverse profiles on noise. Remington and Webb reported theoretical results showing that conforming profiles could lead to a reduction in noise generation. Dings and Dittrich reported experimental results which showed apparently inconsistent roughness-to-noise behaviour between wheels with different braking systems. They suggested that these results could be explained by an increase in noise for a given roughness level when the profiles are conforming. This paper describes a new analytical investigation of the effects of transverse profiles which aims to resolve this conflict. It is based on new very detailed roughness measurements. The data were analyzed first using a discrete point reacting spring model (DPRS). The transverse profiles of the wheel and rail were replaced with circular transverse profiles of different radii of curvature. It was found that the average roughness across the contact zone decreased as the width of this zone was increased, but that these reductions were only modest. The DPRS predictions showed little or no decrease in interaction force with increasingly conforming profiles. The TWINS model has been used to perform calculations which confirmed that, for the roughness data examined, little noise reduction benefit could be expected from a conforming wheel, and in some circumstances it could lead to an increase in noise. TWINS was also used to study the effects of the actual transverse profiles in an attempt to explain more fully the measured results. Some useful conclusions are drawn, but a full explanation of the measured results has not yet been obtained as all three types of braking system lead to some degree of conforming profiles.

1. INTRODUCTION

The static loading due to the vehicle causes local elastic deformation of the wheel and rail so that contact occurs over a small area, typically 10–15 mm in size. Irregularities of the wheel and rail surface (roughnesses) induce dynamic forces at the contact region that excite the wheel and rail into vibration and as a result they

0022-460X/00/130537 + 12 $35.00/0

radiate noise. Theoretical models accounting for these phenomena are well developed and have been extensively validated [1–6]. However, the effect of the contact geometry on noise generation is not wholly understood, particularly where the transverse wheel profiles exhibit hollow wear.

Two recent papers reported apparently conflicting results relating to the effects of transverse profiles on noise. Remington and Webb [7] reported theoretical results showing that conforming profiles could lead to a reduction in noise generation, because the contact patch width is increased. If the roughness is sufficiently uncorrelated in the direction transverse to rolling this would lead to reduced wheel/rail interaction forces and radiated noise. Dings and Dittrich [8], on the other hand, reported experimental results which showed apparently inconsistent roughness-to-noise behaviour between wheels with different braking systems. The smoothest wheels, which had disc brakes with supplementary sinter blocks, were not the quietest. It was suggested that these results could be explained by an increase in noise for a given roughness level when the profiles are conforming, as these wheels appeared on visual inspection to have a greater degree of hollow wear than the others. This paper describes a new analytical investigation of the effects of transverse profiles which aims to resolve this conflict.

2. MEASUREMENT DATA

To provide a basis for the analysis described here, new, very detailed roughness measurements were carried out by Netherlands Railways and TNO Institute of Applied Physics on a series of nine nominally identical 920 mm diameter wheels. These are of the same design as most of the wheels measured in reference [8]. They had various levels of wear and represented three different braking systems: disc

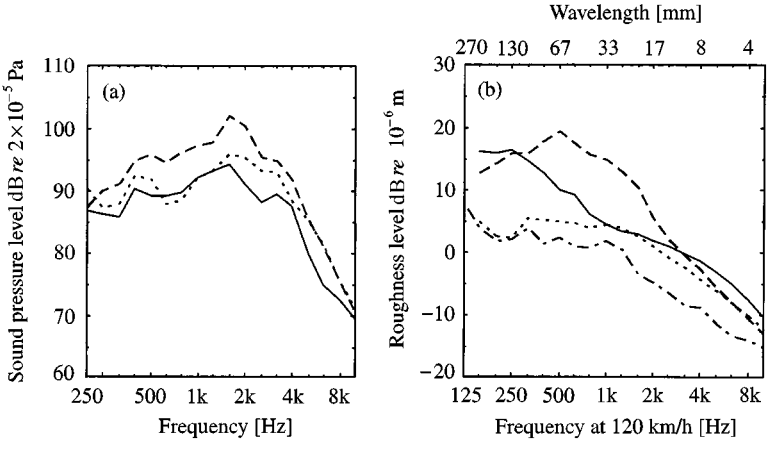

Figure 1. Comparison of wheels with different braking systems. (a) Average sound pressure measured at 1 m from the rail and 0·5 m above the top of the railhead: ——, disc brakes only, 101·6 dB (A); – – –, cast-iron block brakes, 108·3 dB (A); ·····, sinter block brakes, 103·7 dB (A). (b) Average roughness for wheels of each type of braking system and for the rail (– · – ·).

brakes with supplementary cast-iron blocks, supplementary sinter blocks and supplementary magnetic rail brakes. The roughness of each wheel was measured on at least 25 parallel lines spaced 2 mm apart across the running surface, and sampled at 0·5 mm intervals around the circumference. Corresponding transverse profiles were also measured. The noise from these individual wheels was measured by a series of microphones at 1 m from the nearest rail as the trains passed at 120 km/h on their first journey after roughness measurement. The rail roughness and transverse profile were also measured at the test site.

The average sound pressure spectrum for the test wheels with each type of braking system is shown in Figure 1(a). Figure 1(b) shows the corresponding average roughness spectra for the central 20 mm region of the running surface. No contact filtering has been applied, but large pits in the surface have been removed from the time-series data (see reference [9]). As in reference [8] the wheels with cast-iron blocks are the noisiest and those with only disc brakes are the quietest. The wheels with sinter blocks are the smoothest.

3. EFFECT OF TRANSVERSE PROFILE RADIUS

3.1. DISCRETE POINT REACTING SPRING MODEL

As in reference [7], use has been made of a discrete point reacting spring model (DPRS). This is described in detail in reference [10] along with a validation against a more rigorous Boussinesq procedure. The DPRS model represents the contact zone as a two-dimensional array of independent springs. In order to ensure that the overall contact stiffness and contact patch dimensions are preserved, the individual springs are non-linear and adjustments are required to the radii of curvature of the wheel and rail surfaces. The measured roughness is then introduced between the wheel and rail and a blocked force is calculated in the spatial domain assuming the wheel and rail to be rigid. This can then be Fourier transformed into the inverse wavelength domain, or for a given train speed, the frequency domain.

In order to study the effect of profile modifications, the transverse profiles of the wheel were replaced with circular transverse profiles with radii of curvature, R_{wt}, ranging from ∞ (coned) to 305 mm, in combination with a rail transverse radius of curvature, R_r, of 300 mm. Example results are shown in Figure 2. For these cases, with a static wheel load of 40 kN, the contact patch has dimensions $10{\cdot}4 \times 8{\cdot}0$ mm for the coned profile and $6{\cdot}7 \times 25{\cdot}0$ mm for the conforming profile, the first dimension applying in the rolling direction. The respective contact stiffnesses are $1{\cdot}06 \times 10^9$ and $1{\cdot}66 \times 10^9$ N/m.

The predictions from the DPRS model generally show a small increase in wheel/rail interaction force with increasingly conforming wheel profiles. This is because, although the average roughness across the contact zone tends to decrease as the width of this zone is increased, these reductions are only modest. Moreover, the blocked force is influenced by the contact stiffness, the higher contact stiffness for a conforming profile resulting in the blocked force increasing, as seen in Figure 2. An equivalent roughness can be derived from the blocked force divided by

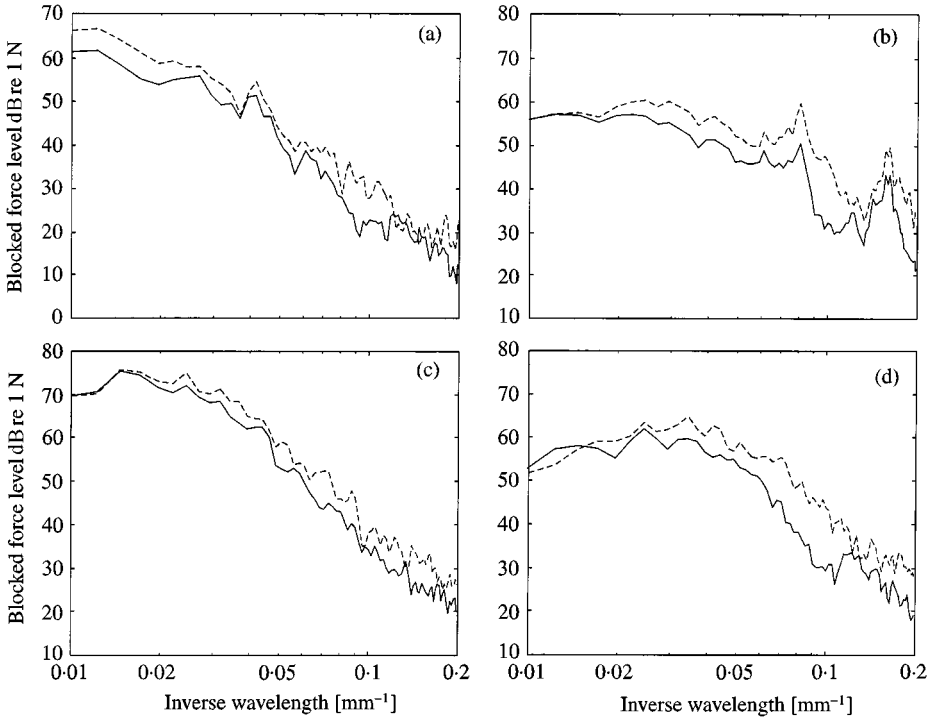

Figure 2. The estimated blocked force for a rail of transverse radius 300 mm: ——, coned wheel profile; - - -, conforming wheel with 330 mm transverse radius. (a) rail roughness, (b) disc-braked wheel, (c) wheel with cast-iron brake blocks, (d) wheel with sinter brake blocks.

the average contact stiffness. This is found to be almost unchanged for these profile changes, apart from the sinter block-braked wheel where it increases particularly between inverse wavelengths of 0·05 and 0·1 mm^{-1}.

3.2. TWINS CALCULATIONS

Calculations have been performed using the TWINS model for rolling noise [5, 6] for the wheel and track types corresponding to the measurements. The equivalent roughnesses derived from the DPRS calculations are used as inputs. Changing the wheel or rail transverse profiles has two different effects within the TWINS calculation. Firstly, as already accounted for in the DPRS calculations, the equivalent roughness is modified by the averaging effect of the contact zone. Secondly, there is an additional effect on the wheel/rail interaction due to the change in contact patch dimensions. This mainly affects the contact stiffness, a high contact stiffness resulting in increased vibration of the wheel and rail [4]. The results are summarized in Table 1 which lists the change in overall A-weighted sound power level. These results show that there is an increase in noise in each case for the conforming wheel.

TABLE 1

Difference in predicted A-weighted sound power level for $R_{wt} = 330\,mm$ *versus* $R_{wt} = \infty$

Roughness	Effect of contact receptances (dB)	Change in roughness filtering (dB)	Overall effect (dB)
Rail roughness	1·4	0·8	2·2
Disc-braked only	1·6	3·4	5·0
Cast-iron block brakes	1·4	0·2	1·6
Sinter block brakes	1·4	4·0	5·4

4. PARAMETRIC STUDY

In the remainder of the study, the actual transverse profiles have been analyzed in an attempt to explain more fully the measured results. The strongly conforming profiles limit the applicability of the DPRS model, as the radius of curvature is not constant across the contact zone. This means that the correction required to form equivalent radii of curvature to ensure the correct contact patch dimensions cannot easily be applied. Instead, a parametric study using TWINS has been performed to determine which parameters have most effect on the radiated noise in order to deduce by indirect means the effects of transverse profiles on noise.

4.1. LATERAL CONTACT POSITION

In a railway system the wheelsets are free to move laterally relative to the track, constrained only by their flanges. The wheelset location on the rail during the experiments is therefore unknown. By matching the transverse profiles of the wheels and rails, the contact location can be plotted as a function of wheelset lateral displacement. An example is shown in Figure 3. From these contact locations on each wheel, the rolling radius difference could be calculated as a function of wheelset lateral displacement. "Stable" wheelset positions correspond to a rolling radius difference of zero. For wheelsets with hollow wear, two such positions usually exist. These positions are identified in Figure 3.

For each stable wheelset position the corresponding location of the contact on the wheel and rail surface is plotted in Figure 4 relative to their nominal positions. The contact position varies from the nominal positions between -35 and $+35$ mm on the wheel and between -30 and $+20$ mm on the rail. There is roughly a linear relationship but not a 1:1 correspondence, due to the lateral movement of the wheelset. No points are found in the Figure in the region near the nominal contact positions.

As a result of the differences in these contact positions, the excitation of the wheel/rail system will differ from one wheel to another. Generally, when the contact

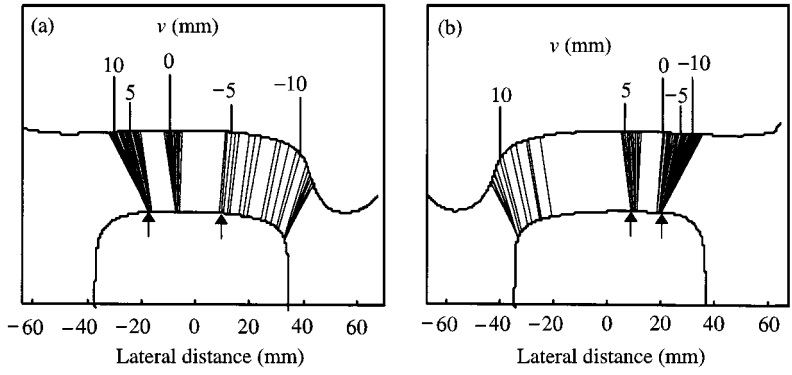

Figure 3. Example of contact position on wheel and rail as a function of lateral wheelset position—wheel with supplementary cast-iron block brakes. Lines join corresponding contact positions on wheel and rail surfaces. Arrows indicate stable positions. (a) left wheel and rail, (b) right wheel and rail.

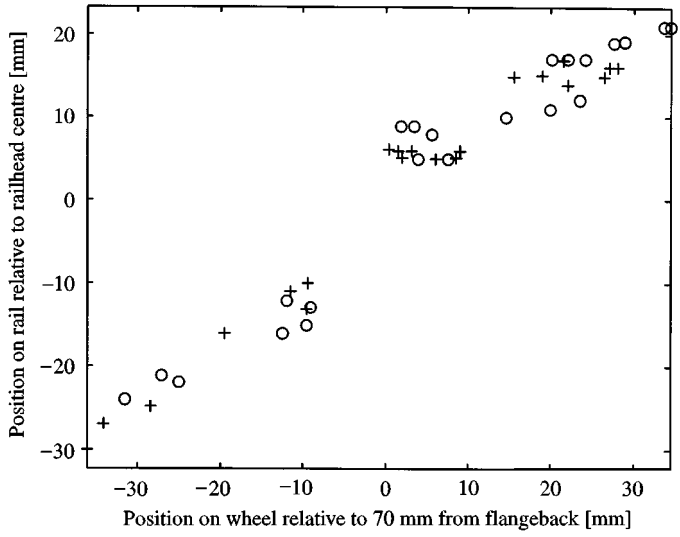

Figure 4. Position of the centre of the contact zone on the wheel and on the rail for the stable wheelset positions. + indicates left-hand wheel, ○ indicates right-hand wheel (side of noise measurements). Positive is towards the outside of the track.

point is further from the nominal position, greater excitation of lateral components of vibration can occur and therefore greater noise radiation will ensue. Calculations using the TWINS model have been performed for 18 combinations of wheel and rail contact position typical of those represented in Figure 4. Apart from the contact position, all other input parameters are kept constant. A single roughness spectrum—the cast-iron block braked spectrum from the DPRS analysis with coned profile—has been used in all cases to provide a consistent basis for comparison. The overall A-weighted sound level for these cases varies by up to 4 dB

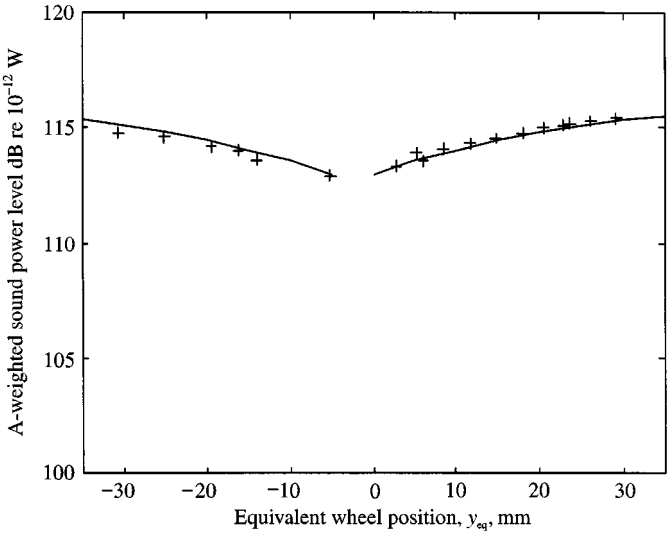

Figure 5. TWINS predictions of sound power for various positions of the centre of the contact zone on the wheel and on the rail (roughness from cast-iron block-braked wheel). The sound level is plotted against the equivalent wheel position, y_{eq}. Also shown is a quadratic regression line fitted as a function of $|y_{eq} + 2{\cdot}5|$.

compared to that for the contact near the centre. Figure 5 shows this level plotted against an equivalent contact position, y_{eq} constructed from the contact position on the wheel (y_w) and the rail (y_r) on the basis of a regression line through the results of Figure 4: $y_{eq} = 0{\cdot}64\, y_w + 0{\cdot}48\, y_r + 0{\cdot}466$ (mm). At $y_{eq} = -2{\cdot}5$ mm, i.e., close to the nominal contact point, a minimum occurs for this wheel/track combination.

These results have been used to estimate the noise for the various stable positions given in Figure 4. Grouping these results according to braking system allows an estimate to be made of the average noise level for each type of braking system, apart from its roughness, i.e., the effect on noise level of lateral contact position. It is found that the sets of wheels tested with different braking systems have only slightly different mean contact positions, so the mean results for the three types of braking are within 0·4 dB of each other, whereas the standard deviation in each set is 0·7 dB. Therefore, although the contact position has a significant effect on the noise radiated, it cannot, by itself, explain the differences in roughness-to-noise behaviour found between wheels with different braking systems.

4.2. CONTACT STIFFNESS

Roughness excites the wheel/rail system by introducing a vertical relative displacement at the contact zone. This produces rail vibration, wheel vibration and local elastic deformation of the contact zone, the proportions of each depending on their point receptances [4]. The predicted vertical receptance amplitudes of the

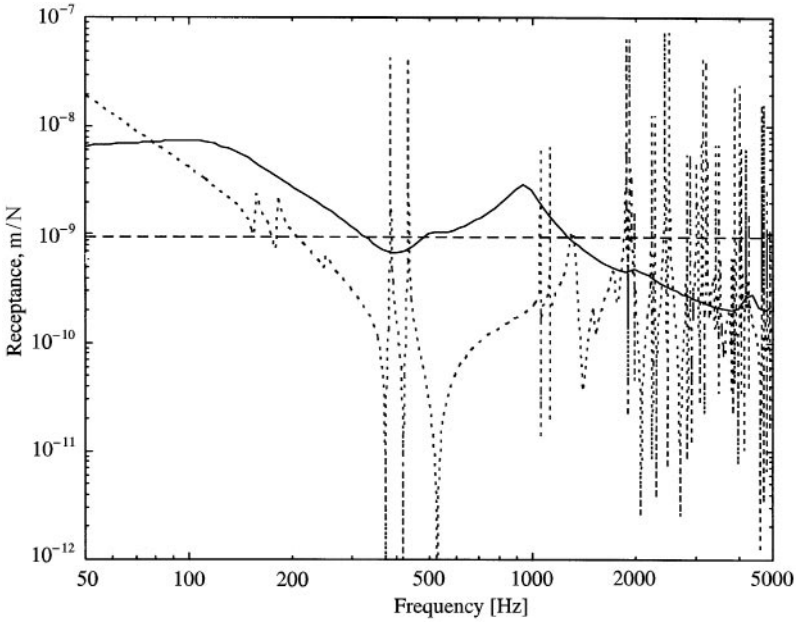

Figure 6. Vertical point receptances of the rail (— —), the wheel (· · · · ·) and the contact spring (– – –) predicted by TWINS.

wheel, the rail and the contact spring are shown in Figure 6 for the example case considered here. The wheel receptance applies to a rotating wheel as seen from the contact zone, so that the resonances generally appear in pairs. It can be seen that, between 100 and 1000 Hz, apart from around 400 Hz, the rail has the highest receptance and will therefore vibrate with an amplitude close to that of the roughness [4]. At high frequencies, the wheel has the highest receptance near its resonances, but elsewhere the contact spring has the highest receptance. In these bands between the wheel resonances, the contact spring will therefore absorb most of the roughness.

By lowering the contact stiffness, the receptance of the contact spring is increased, and a greater part of the roughness excitation is absorbed by the contact zone. This brings about a reduction in the wheel and rail vibrations and hence the noise radiated. In order to quantify this effect, the TWINS model has been used to perform calculations in which the contact stiffness has been modified, all other parameters being kept the same. The roughness spectrum used is again based on the wheel roughness for cast-iron block-braked wheels. The overall predicted sound power levels are shown in Figure 7. Further decrease in contact stiffness will result in reductions almost proportional to $20\log_{10}(k_H)$ as the contact receptance becomes greater than that of the rail or wheel for stiffnesses below 10^8 N/m. On the other hand, further increase in contact stiffness above 10^{10} N/m will produce negligible increases in noise as the contact receptance becomes small compared to those of the wheel or rail, except near wheel anti-resonances. The results predicted in section 3 for varying wheel transverse radius correspond to a relatively small change in contact stiffness (see the first column of Table 1).

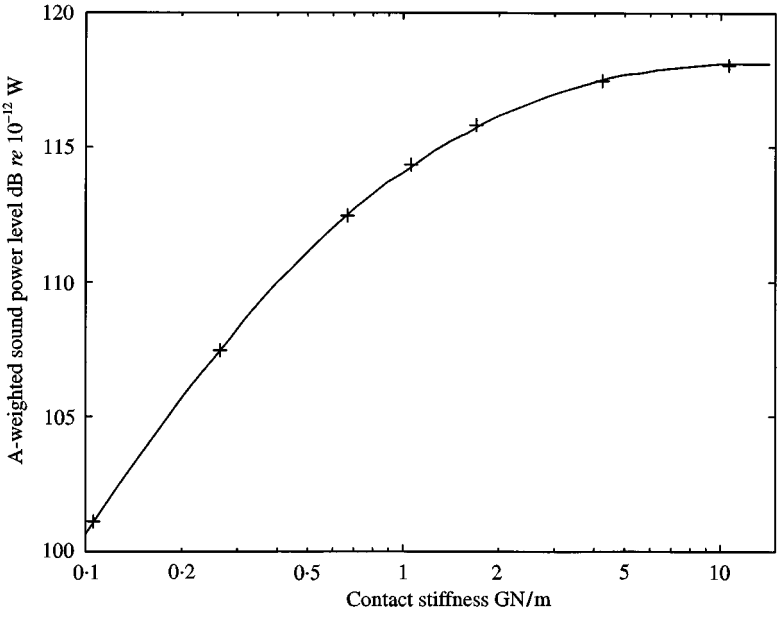

Figure 7. TWINS predictions of A-weighted sound power level for various values of contact stiffness. Roughness is from cast-iron block-braked wheels, coned profile processed by DPRS model. Nominal contact stiffness is 1·06 GN/m.

4.3. EQUIVALENT RADII OF CURVATURE

In order to estimate the contact stiffness for the actual transverse profiles, without resorting to non-Hertzian contact calculations, an equivalent radius of curvature near the contact is studied. This depends on the wheelset lateral position. For each wheel, the approximate transverse radius of curvature which applies at the wheel/rail contact point has been determined by fitting a quadratic function to the difference between the wheel and rail profiles over a width of 10 mm around the nominal contact point (point of first contact as shown in Figure 3).

These radii of curvature are generally quite large towards the centre of the wheelset motion, up to 1500 mm and become small towards the extremes, particularly where flange contact occurs where radii smaller than 10 mm occur. At the stable wheelset locations for each wheel, it is found that, in most cases, one wheel has a small, and the other a large radius of curvature. Thus, the radii of curvature at the stable wheelset positions can be grouped into two sets. Average radii of curvature for each type of braking system have been determined for the larger radii and for the smaller ones. These are converted into equivalent transverse radii of curvature R_{eq} defined by $1/R_{eq} = 1/R_{wt} + 1/R_r$ where R_r and R_{wt} are each taken as positive for convex surfaces. Values of R_{eq} are found between about 30 and 750 mm at the stable wheelset locations.

In order to gain an impression of the likely contact patch dimensions for these non-Hertzian contacts, the above radii of curvature have been used in a Hertzian contact calculation. The corresponding contact stiffness and dimensions of the

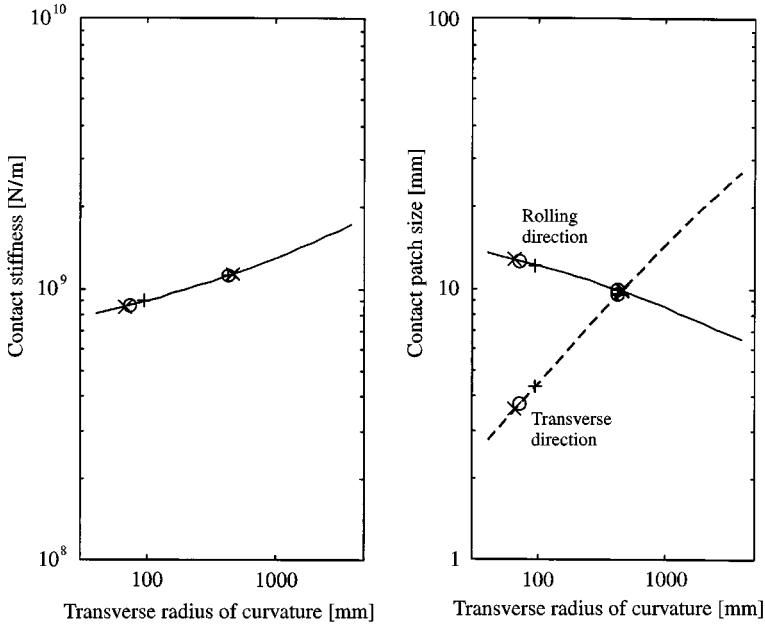

Figure 8. Dependence of contact stiffness and contact patch major and minor diameters on effective transverse radius of curvature at the wheel/rail contact, R_{eq}. Symbols show results for average "most likely" wheelset positions for each type of braking system: + , disc-braked; ○, cast-iron block; ×, sinter block.

contact ellipse are shown in Figure 8. The lower equivalent transverse radii, found for contact near the flange/gauge corner, result in a contact patch only slightly longer in the rolling direction than for contact in the centre of the rail head and a contact stiffness only slightly lower. The transverse dimension, on the other hand, is approximately halved.

The change in contact stiffness for this range of radii of curvature is quite small, the minimum and maximum values having a factor of only 1·3 between them. The change in noise level can be seen from Figure 7 to be quite small for such a change in contact stiffness and is limited to about ± 1 dB.

4.4. OTHER PARAMETERS

In this section some other parameter changes are discussed briefly.

Changes to the contact patch dimensions lead to changes in the creep force terms linking the wheel and rail in the lateral direction. In order to study this effect, the TWINS model has been run for a series of cases in which the creep terms linking lateral wheel and rail vibration have been changed by factors of between 0·1 and 10 whilst all other parameters have been kept constant. The effect on noise is found to be extremely small, less than 0·1 dB. Moreover, the change in creep terms for the various radii of curvature considered in the previous sections is small compared to the range covered, typically only a factor of 1·5.

From the wheel and rail profiles, the angle which the contact surface makes with the horizontal is found to remain mostly within the range $\pm 3^{\circ}$. The effect of this variation in contact angle on noise has been predicted and found to be less than 0·2 dB. For larger contact angles such as occur with flange contact, the effect will be greater, but this has not been quantified.

For the worn wheel profiles, at many of the stable contact positions on the wheel and rail the nominal contact position can move across the wheel or rail surface by 30 mm or more for a small wheelset deflection (see Figure 3). As the wheel profiles are not constant around the perimeter and the rail profiles also vary along the track it is quite likely that the centre of the wheel/rail contact will oscillate between stable positions up to 30 mm apart even if the wheelset displacement did not vary.

This lateral oscillation of the effective point of contact can induce significant moment excitation of the wheel/rail system. An initial consideration of this phenomenon in reference [4] suggested that it could be a significant additional excitation mechanism. At that time there were no measured results to indicate the likely extent of this effect, but the measured data here could be used for this purpose. The lateral movements of contact position here, of the order of 30 mm, are greater than assumed in reference [4]. This suggests that this could indeed be a significant source of excitation, particularly at lower frequencies. Moreover, the potential lateral motion of the contact is found to be appreciably greater for the wheels with sinter block braking than the other wheels. A full analysis of the likely effect has still to be carried out.

5. CONCLUSIONS

Detailed roughness measurements of wheels and rail have been used in conjunction with the DPRS model for contact behaviour and the TWINS model for rolling noise. It was found from analysis using the DPRS model that, although the average roughness across the contact zone decreased as the width of this zone was increased, the wheel/rail interaction force increased for conforming wheel profiles. TWINS calculations, using these results as inputs, confirmed that little noise reduction benefit could be expected from the conforming wheel, because the negative effect of the higher contact stiffness was not sufficiently compensated by the averaging over a wider contact zone. In some cases, notably the wheels with sinter brake blocks, the equivalent roughness is actually increased by the averaging over a wider contact zone, as the roughness was higher towards the edge than in the central running zone. This is a partial explanation of the measured results in reference [8].

A number of parameters have been studied in an attempt to explain the measured results further. The average contact patch positions on the wheel/rail surfaces were found to have a moderate influence on the noise. The sensitivity to the contact stiffness was also investigated but found to have only a small effect in the range of actual profiles. Lateral displacement of the contact relative to the nominal position leads to an increase of up to 4 dB but no significant differences were found between the wheels with different braking systems. The most likely explanation for

remaining discrepancies between predicted and measured results appears to be the excitation of the wheel/rail system by an additional moment due to transient variations in the nominal contact position.

ACKNOWLEDGMENT

The authors are grateful to the European Rail Research Institute who funded this work and to the TNO Institute of Applied Physics (represented by Marcel Janssens) who managed it on their behalf. The new measurement data were obtained by Netherlands Railways and TNO Institute of Applied Physics within the framework of a European Union Brite-Euram project, Silent Freight. Their assistance is gratefully acknowledged.

REFERENCES

1. P. J. Remington 1976 *Journal of Sound and Vibration* **46**, 419–436. Wheel/rail noise, Part IV: rolling noise.
2. P. J. Remington 1987 *Journal of the Acoustical Society of America* **81**, 1805–1823. Wheel/rail rolling noise, I: theoretical analysis.
3. P. J. Remington 1987 *Journal of the Acoustical Society of America* **81**, 1824–1832. Wheel/rail rolling noise, II: validation of the theory.
4. D. J. Thompson 1990 *Ph.D. thesis, University of Southampton.* Wheel/rail noise-theoretical modelling of the generation of vibrations.
5. D. J. Thompson, B. Hemsworth and N. Vincent 1996 *Journal of Sound and Vibration* **193**, 123–135. Experimental validation of the TWINS prediction program for rolling noise, Part 1: description of the model and method.
6. D. J. Thompson, P. Fodiman and H. Mahé 1996 *Journal of Sound and Vibration* **193**, 137–147. Experimental validation of the TWINS prediction program for rolling noise, Part 2: results.
7. P. J. Remington and J. Webb 1996 *Journal of Sound and Vibration* **193**, 335–348. Wheel/rail noise reduction through profile modification.
8. P. C. Dings and M. G. Dittrich 1996 *Journal of Sound and Vibration* **193**, 103–112. Roughness on Dutch railway wheels and rails.
9. D. J. Thompson 1996 *Journal of Sound and Vibration* **193**, 149–160. On the relationship between wheel and rail surface roughness and rolling noise.
10. P. J. Remington and J. Webb 1996 *Journal of Sound and Vibration* **193**, 83–102. Estimation of wheel/rail interaction forces in the contact area due to roughness.